

Controlling the distribution of UAVs using artificial pheromone tags: Parameter Tuning

Ján Zelenka¹[0000-0001-5852-0429], Tomáš Kasanický¹[0000-0002-1931-6537],
Nayden Chivarov²[0000-0002-3629-8107]

¹ Institute of Informatics, Slovak Academy of Sciences, Dúbravská cesta 9, Bratislava 84507, Slovakia

² Institute of Information and Communication Technologies, Bulgarian Academy of Science, Sofia, Bulgaria

jan.zelenka@savba.sk, tomas.kasanicky@savba.sk

Abstract. As a result of global warming and changing climate conditions, we are facing increasingly severe weather fluctuations. In addition to other disasters, large-scale fires are occurring more frequently. One of the important means of fighting fires is their monitoring. This work offers a framework focused on long-term, scalable automated monitoring of areas of interest. The basic idea is to use swarms of autonomous drones that behave like reactive agents. They are coordinated only using pheromone marks and, in this way, ensure optimal long-term spatial distribution. The article describes the swarm setup and the evaluated experiments.

Keywords: monitoring, swarm coordination,

1 Introduction and problem description

This article continues the research on the coordination of a group of unmanned aerial vehicles (UAVs) in space monitoring as a solution for fire prevention, which is the subject of the EU SILVANUS project under the Green Deal (SILVANUS, 2023) [1] and the national project SILVANUS-SK.

The SILVANUS project consists of several work packages and tasks, from the design and implementation of the cloud infrastructure to the collection and storage of distributed data from sensors, social networks, and satellites. One of the co-investigating tasks is the coordination of a group of unmanned aerial vehicles (UAVs) during phase “(Prevention and Preparedness before the wildfire)”, supported by the fire risk. Currently, fire monitoring is provided by field patrols, especially during the declared period of increased fire risk. The fire danger assessment is not provided at the local or regional levels, but only at the national level. For this purpose, the meteorological fire danger index (FDI) is used, calculated according to the Baumgartner formula. Satellite data, when supplemented with forestry data (e.g., blue areas in Fig. 1) and manual field data collection, can yield a more accurate fire danger index for a given area, enabling it to be divided into smaller sub-areas with different risk values. At this stage, the role of the

drones is to monitor (continuously or on demand) specific areas, covering areas directly proportional to the fire danger index rating. Swarm robotics and unmanned aerial vehicles (UAVs) are currently expanding rapidly across many application areas, especially where conventional approaches are too expensive or time-consuming.

Swarm robotics and autonomous unmanned aerial vehicles (UAVs) are currently expanding rapidly across many areas, especially where conventional approaches are too expensive or time-consuming. One such area is the use of UAVs for forest fire prevention and monitoring. The availability of suitable robotic equipment with sensors and control systems is a major factor in the development of this type of application. The current state of continuous forest fire monitoring is described in scientific studies [5-8], which use unmanned aerial vehicles. Study [6] describes the importance of swarms and nature-inspired methods for coordinating a swarm (20 UAVs) to cover large areas, aiming to detect fires at an early stage. Study [8] extends the addressed issue and points to the use of digital twin technology for forest stand monitoring. The Finnish Center for Artificial Intelligence [2, 9] is dedicated to fire monitoring using swarms, but it has not yet been tested on real hardware platforms. As part of the SILVANUS project, one task is to design a forest stand monitoring system before, during, and after a fire using swarm UAV technologies. As part of the project, a pilot demonstration was also carried out in the Slovak Republic and the Czech Republic, where other regulatory and legislative restrictions had to be considered (e.g., registration with the Slovak Transport Authority and a licensed pilot required). The legislation does not recognize flying in a group (or controlling multiple drones at once by one operator), although modern commercial solutions (e.g., from DJI) already offer this [3, 4, 11].

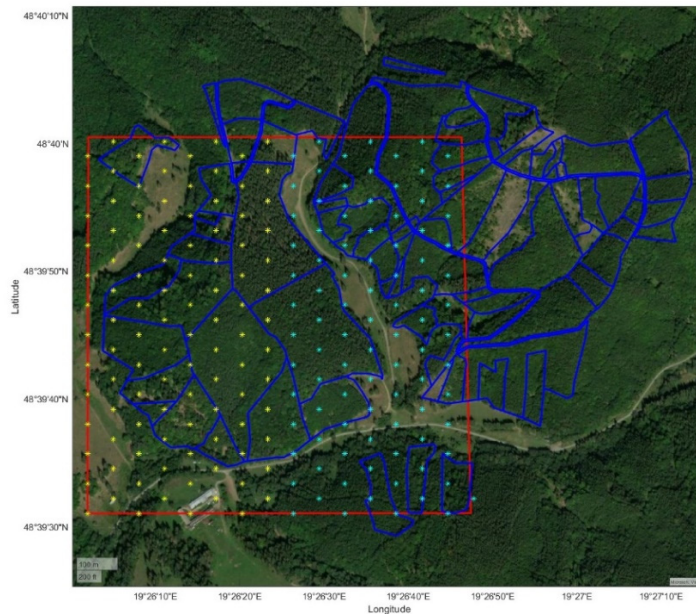


Fig. 1. Real testing environment, 196 points of interest, FDI = 1 (yellow points) and FDI = 2 (turquoise points) in a ratio of 55% to 45%.

2 Algorithm description And Experiments

2.1 Algorithm description

The algorithm design is based on our previous studies, where artificial pheromone marks are used for adapting a heterogeneous swarm in monitoring tasks [10]. It has been proven in publications [10] that it is able to successfully control three basic behaviors: space exploration, population management, and transportation. All these properties are combined in a single algorithm meaning that the behaviors were running simultaneously and space exploration (the main goal) was never stopped or interrupted. The algorithm was shown to be robust, fault tolerant, and independent of the environment where the swarm worked. The swarm of agents adjusted its size autonomously accordingly to the size of the space to be explored and the optimal population size was reached in a finite time. The algorithm is designed for a swarm of robots that follow identical local behavioral rules and operate without any supervisory control. Therefore, the robots must be able to accomplish the target task autonomously, without centralized intervention, while remaining scalable with respect to the population size, so that the task can be performed by a single robot as well as by multiple robots with increasing efficiency. The advantage of this solution is that the goal can be achieved even in the event of a random failure of other agents without the intervention of any superior authority. Therefore, this publication is focused on using these pheromone marks to monitor areas more frequently but evenly according to environmental requirements. The goal is to achieve algorithm settings so that places with higher FDI are visited more frequently and directly proportional to the value of the FDI. Since robots in a group have the same rules and coordinate only based on mutual communication via a pheromone trail, which fades over time, it is necessary to set the algorithm parameters appropriately. When choosing a location or direction of movement that the device will visit, it decides between:

- influence of the pheromone marks value in its surroundings, the o_{FER} value;
- influence of the fire danger index of individual points, the o_{FDI} value;
- influence of the direction of rotation compared to the upstream direction (i.e., rectilinear movement is preferred due to the efficiency of the UAV flight versus frequent sharp yaw).

The robot's movement is controlled based on unambiguous rules that are identical for all members of the swarm:

- A robot calculates the suitability S_i of each point in its field of view separately. This suitability determines the probability with which the robot can reach a given point. The selection of points is random but influenced by their suitability S_i .
- When the robot reaches the target point, it leaves a pheromone trail (or sends a broadcast message) and adds the pheromone value to its internal map.
- On its way to the target, the robot checks whether there is a risk of collision with another robot; in the event of a collision, one of them avoids the other (assumption of functionality integrated into individual UAVs).

The suitability S_i of the i^{th} point is calculated according to the formula (1), where:

- the first part of the formula prefers the point with the lowest pheromone FER , the o_{FER} parameter ensures the influence of the pheromone;
- the second part of the formula prefers the point with the highest FDI index - the goal is for the area with the higher FDI to be visited more often, the o_{FDI} parameter ensures the influence of the pheromone;
- the third part of the formula prefers the point with the smallest deviation from the current flight direction - this parameter ensures in-depth search, but also depends on the UAV devices used and their flight characteristics (we consider the use of multi-rotor UAVs where changing the trajectory is not very energy-intensive). The o_{angle} parameter ensures the influence of the pheromone.

$$S_i = \left(o_{FER} * \left(1 - \frac{FER_i}{\max(FER)} \right) \right) + \left(o_{FDI} * \left(1 - \frac{FDI_i}{\max(FDI)} \right) \right) + \left(o_{angle} * \left(\frac{1 - \text{angle}_i}{\max(\text{angle})} \right) \right) \quad (1)$$

Each robot stores information in its own pheromone map, which is modified:

- by receiving a broadcast message from another robot, mainly an increase in FR value by a constant amount.

$$FM_i(t) = FM_i(t - 1) + FR \quad (2)$$

- at regular intervals depending on the FDI_i value, by the following formula

$$FM_i(t) = FM_i(t - 1) - OV * FDI_i \quad (3)$$

where OV represents the constant value which may influence the impact of fire risk variation

2.2 Experiments 1 - simple environment 196 point of interest, 3x UAV moving 5 meters per second, simulation duration 20000 seconds

The aim of the experiment is to determine the dependence between o_{FER} and o_{angle} . The first experiment was conducted in an environment with the same value of the FDI , therefore the parameter o_{FDI} was set to $o_{FDI} = 0$. The aim of the experiment was to confirm the assumption that the space would be searched and to determine the impact of these parameters.

Each simulation was set for a duration of 20000 seconds, with agents moving at a constant speed of 5 m/s. For each experiment (a given combination of parameters o_{FER} , o_{FDI} , o_{angle}), five repetitions were performed and the arithmetic mean was calculated in the resulting table. For a given space, 196 points were designed at which a photograph was to be taken (with the required overlap and regardless of the agent's flight direction). To evaluate the settings, we determined the maximum and minimum number of visits to a given location, how many locations were visited (marked as PNB value in table on the Fig. 2), the average number of point visits, and the quantile values Q10 and Q90 of

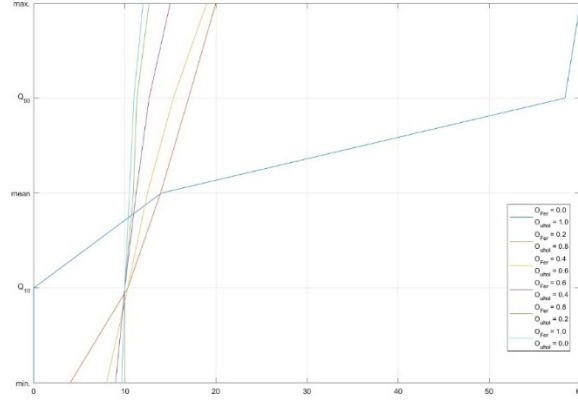


Fig. 3. Graphical representation of the result when setting FR=100, OV = 0,05 (top left setting on the Fig. 2.).

The comparisons with deterministic strategies requiring global planning, such as uniform area coverage, are not well suited. Instead, we consider simple decentralized baseline strategies as relevant references, namely random motion, where a robot randomly selects a free neighboring point at each step, and billiard motion, in which a robot follows a chosen direction until it encounters an obstacle and then randomly selects a new direction (this case also represents a situation where the influence of o_{angle} is at a value of 1). A comparison of the proposed approach with these baseline behaviors is presented in the Fig. 5 (for the comparison a 15 repetition per setting was done, simulation duration SD of 20000 and 40000 seconds was set).

O _{angle}	OV = 0.05						OV = 0.15						OV = 0.25					
	0.00	0.20	0.40	0.60	0.80	1.00	0.00	0.20	0.40	0.60	0.80	1.00	0.00	0.20	0.40	0.60	0.80	1.00
max	64,00	15,20	13,80	12,80	12,40	12,00	71,00	12,60	12,40	12,00	12,40	12,00	85,00	17,40	17,00	16,40	16,20	16,20
Q90	62,80	13,20	12,40	12,00	12,00	11,40	69,40	12,00	11,00	11,00	11,38	11,00	83,20	15,40	14,60	14,38	14,40	14,00
mean	14,03	11,62	11,30	11,34	11,13	10,92	14,03	10,68	10,48	10,51	10,37	10,37	14,03	11,31	11,11	10,92	10,95	11,14
Q10	0,00	10,00	10,20	11,00	11,00	10,40	0,00	9,40	9,40	9,40	9,40	9,42	0,00	8,62	7,20	7,60	7,20	7,44
min	0,00	8,60	9,40	10,20	10,20	10,00	0,00	7,80	7,80	7,20	8,40	7,80	0,00	4,20	4,20	4,60	3,60	4,60
PBN	85,90	196,00	196,00	196,00	196,00	196,00	85,90	196,00	196,00	196,00	196,00	78,80	196,00	196,00	196,00	196,00		
(95%CI) max	64,00 ± 0,00	15,20 ± 0,56	13,80 ± 0,56	12,80 ± 0,56	12,40 ± 0,68	12,00 ± 0,80	71,00 ± 43,46	12,60 ± 0,68	12,40 ± 0,68	12,00 ± 0,00	12,40 ± 0,68	12,00 ± 0,00	85,00 ± 23,80	17,40 ± 1,11	17,00 ± 0,88	16,40 ± 1,11	16,20 ± 1,04	16,20 ± 0,56
(95%CI) mean	14,03 ± 0,01	11,62 ± 0,33	11,30 ± 0,30	11,34 ± 0,24	11,13 ± 0,28	10,92 ± 0,24	14,03 ± 0,01	10,68 ± 0,17	10,48 ± 0,10	10,51 ± 0,15	10,37 ± 0,16	10,37 ± 0,11	14,03 ± 0,02	11,31 ± 0,28	11,11 ± 0,28	10,92 ± 0,18	10,95 ± 0,07	11,14 ± 0,08
(95%CI) min	0,00 ± 0,00	8,60 ± 0,56	9,40 ± 0,68	10,20 ± 0,56	10,20 ± 0,56	10,00 ± 0,00	0,00 ± 0,00	7,80 ± 0,56	7,80 ± 0,56	7,20 ± 1,62	8,40 ± 0,68	7,80 ± 1,04	0,00 ± 0,00	4,20 ± 0,64	4,20 ± 1,04	4,60 ± 1,42	3,60 ± 2,26	4,60 ± 0,68
(95%CI) PBN	85,90 ± 25,48	196,00 ± 0,00	196,00 ± 0,00	196,00 ± 0,00	196,00 ± 0,00	196,00 ± 0,00	85,90 ± 49,82	196,00 ± 0,00	196,00 ± 0,00	196,00 ± 0,00	196,00 ± 0,00	196,00 ± 0,00	78,80 ± 29,83	196,00 ± 0,00	196,00 ± 0,00	196,00 ± 0,00	196,00 ± 0,00	196,00 ± 0,00
max	78,20	15,60	13,60	12,80	12,80	12,60	78,20	13,80	12,40	12,00	12,00	12,20	83,60	12,00	12,00	12,00	16,20	16,20
Q90	68,20	13,40	12,60	12,00	12,00	11,98	75,78	12,58	12,00	11,30	11,30	11,40	82,40	11,40	11,20	11,00	14,40	14,00
mean	14,03	11,80	11,61	11,34	11,37	11,15	14,03	11,31	11,11	10,93	10,85	10,88	14,03	10,74	10,56	10,56	10,95	11,14
Q10	0,00	10,02	10,60	11,00	10,80	11,00	0,00	10,00	10,60	10,40	10,30	10,40	0,00	8,00	8,20	8,20	7,20	7,44
min	0,00	8,60	9,00	10,80	10,20	10,00	0,00	9,00	10,00	10,00	10,20	10,00	0,00	9,40	9,20	9,80	3,60	4,60
PBN	85,90	196,00	196,00	196,00	196,00	196,00	85,90	196,00	196,00	196,00	196,00	84,20	196,00	196,00	196,00			
(95%CI) max	78,20 ± 2,54	15,60 ± 0,68	13,60 ± 0,68	12,80 ± 0,56	12,80 ± 0,56	12,60 ± 0,68	78,20 ± 20,73	13,80 ± 0,56	12,40 ± 0,68	12,00 ± 0,00	12,00 ± 0,00	12,20 ± 0,56	83,60 ± 23,80	12,00 ± 1,11	12,00 ± 0,88	12,00 ± 1,11	16,20 ± 1,04	16,20 ± 0,56
(95%CI) mean	14,03 ± 0,01	11,80 ± 0,20	11,61 ± 0,18	11,34 ± 0,09	11,37 ± 0,12	11,15 ± 0,10	14,03 ± 0,02	11,31 ± 0,24	11,11 ± 0,24	10,93 ± 0,36	10,85 ± 0,23	10,88 ± 0,30	14,03 ± 0,02	10,74 ± 0,28	10,58 ± 0,28	10,58 ± 0,18	10,95 ± 0,07	11,14 ± 0,08
(95%CI) min	0,00 ± 0,00	8,60 ± 0,68	9,00 ± 0,60	10,80 ± 0,56	10,20 ± 0,56	10,00 ± 0,00	0,00 ± 0,00	9,00 ± 0,60	10,00 ± 0,60	10,00 ± 0,00	10,20 ± 0,56	10,00 ± 0,00	0,00 ± 0,00	9,40 ± 1,04	9,20 ± 1,04	9,80 ± 1,42	3,60 ± 2,26	4,60 ± 0,68
(95%CI) PBN	85,90 ± 26,52	196,00 ± 0,00	196,00 ± 0,00	196,00 ± 0,00	196,00 ± 0,00	196,00 ± 0,00	83,40 ± 38,06	196,00 ± 0,00	196,00 ± 0,00	196,00 ± 0,00	196,00 ± 0,00	196,00 ± 0,00	84,20 ± 29,83	196,00 ± 0,00	196,00 ± 0,00	196,00 ± 0,00	196,00 ± 0,00	196,00 ± 0,00

Fig. 4. Graphical representation of the result for stability behavior report for selected setting.

	Random robot motion		Billiard robot motion		FR=200, oFer = 0,6					
					OV = 0.05		OV = 0.15		OV = 0.25	
	SD=20000	SD=40000	SD=20000	SD=40000	SD=20000	SD=40000	SD=20000	SD=40000	SD=20000	SD=40000
max	71,1	170,1	71,2	162,6	12,80	27,90	12,00	26,00	16,40	34,50
Q90	69	167,37	69,09	159,77	12,00	27,00	11,00	25,00	14,38	31,39
mean	14,03	32,03	14,02	32,03622449	11,34	25,86	10,51	23,47	10,92	24,95
Q10	0	0	0	0	11,00	24,90	9,60	21,90	7,60	17,32
min	0	0	0	0	10,20	23,50	7,20	19,30	4,60	12,00
PBN	85,9	88,6	88,2	83,6	196,00	196,00	196,00	196,00	196,00	196,00
(95%CI) max	71,10 ± 0,63	170,10 ± 18,10	71,20 ± 16,93	162,60 ± 26,99	12,80 ± 0,00	27,90 ± 0,23	12,00 ± 0,00	26,00 ± 0,00	16,40 ± 0,00	34,50 ± 0,97
(95%CI) mean	14,03 ± 0,01	32,03 ± 0,01	14,02 ± 0,01	32,04 ± 0,01	11,34 ± 0,00	25,86 ± 0,21	10,51 ± 0,00	23,47 ± 0,06	10,92 ± 0,00	24,95 ± 0,10
(95%CI) min	0,00 ± 0,00	0,00 ± 0,00	0,00 ± 0,00	0,00 ± 0,00	10,20 ± 0,00	23,50 ± 0,38	7,20 ± 0,00	19,30 ± 0,96	4,60 ± 0,00	12,00 ± 0,75
(95%CI) PBN	85,90 ± 11,77	88,60 ± 16,18	88,20 ± 20,58	83,60 ± 13,97	196,00 ± 0,00	196,00 ± 0,00	196,00 ± 0,00	196,00 ± 0,00	196,00 ± 0,00	196,00 ± 0,00

Fig. 5. Graphical representation of the result for baseline comparison on the identical environment conditions (the SD represents duration of the simulation).

2.4 Experiment 3 - simple environment 196 point of interest, FDI 1 and 3 in a ratio of 55% to 45%, 3x UAV moving 5 meters per second, simulation duration 20000 seconds

The third experiment was conducted in an environment where the space was divided into two contiguous parts in a ratio of 55% FDI = 1 and 45% FDI = 3. The aim of the experiment was to examine the influence of individual parameters O_{FER} , O_{FDI} and O_{angle} on the overall search of the space. Each simulation was set for a duration of 20000 seconds, with agents moving at a constant speed of 5 m/s. For each experiment (given combination of parameters O_{FER} , O_{FDI} , O_{angle}), five repetitions were performed and the arithmetic mean was calculated in the resulting table. For illustrative purposes, we show the results for the settings $FR = 200$, $OV = 0.01$. In Fig. 8, the PNB rows are color-coded to indicate where both spaces were fully searched. From the individual results and ratios of the average cell search (mean value in Fig. 8), it can be seen that a ratio of $\frac{1}{3}$ would be achieved with a setting of 0.5 for O_{FER} and O_{FDI} . try to avoid rasterized images for line-art diagram

O_{an}	0	0.1	0.2	0.3	0.4	0.5	0.6	0.7	0.8	0.9	1	
$O_{an}=0$	max	71.0 36.0	72.0 2.0	71.0 35.0	0.0 107.0	36.0 70.0	0.0 107.0	0.0 104.0	0.0 106.0	0.0 106.0	0.0 105.0	0.0 104.0
	Q90	70.0 34.4	70.0 0.0	70.0 33.0	0.0 105.0	35.0 68.0	0.0 105.0	0.0 103.0	0.0 104.0	0.0 103.0	0.0 103.0	0.0 101.0
	mean	17.4 10.2	26.1 0.1	17.4 10.1	0.0 30.3	8.7 20.2	0.0 30.3	0.0 30.3	0.0 30.3	0.0 30.3	0.0 30.3	0.0 30.3
	Q10	0.0 0.0	0.0 0.0	0.0 0.0	0.0 0.0	0.0 0.0	0.0 0.0	0.0 0.0	0.0 1.0	0.0 0.0	0.0 1.0	0.0 0.0
	PNB	33.0 57.0	58.0 7.0	44.0 70.0	0.0 55.0	30.0 81.0	0.0 55.0	0.0 91.0	0.0 67.0	0.0 91.0	0.0 91.0	0.0 81.0
$O_{an}=0.1$	max	26.0 29.0	11.0 49.0	12.0 48.0	8.0 55.0	1.0 66.0	0.0 65.0	0.0 65.0	0.0 62.0	0.0 48.0	0.0 48.0	
	Q90	24.0 27.0	10.0 49.0	10.0 46.0	6.0 53.0	0.0 64.0	0.0 64.0	0.0 62.0	0.0 61.0	0.0 47.0	0.0 37.0	
	mean	12.5 15.7	6.1 23.1	6.5 22.6	3.8 25.8	0.1 30.1	0.0 30.3	0.0 30.3	0.0 30.3	0.0 30.2	0.0 29.1	
	Q10	1.0 0.0	3.0 4.0	3.0 5.6	0.0 7.0	0.0 4.0	0.0 6.0	0.0 8.0	0.0 7.0	0.0 14.0	0.0 20.5	
	PNB	105.0 91.0	105.0 91.0	105.0 91.0	93.0 91.0	100.0 91.0	0.0 91.0	0.0 91.0	0.0 91.0	0.0 91.0	0.0 91.0	
$O_{an}=0.2$	max	19.0 18.0	15.0 26.0	9.0 34.0	2.0 44.0	2.0 46.0	0.0 46.0	0.0 43.0	0.0 40.0	0.0 36.0		
	Q90	18.0 15.4	14.0 25.0	7.0 33.0	1.0 41.0	1.0 43.0	0.0 45.0	0.0 42.0	0.0 37.0	0.0 32.0		
	mean	14.4 13.4	10.6 17.9	5.9 23.3	0.3 29.6	0.2 29.5	0.0 30.2	0.0 30.1	0.0 29.7	0.0 28.2		
	Q10	10.0 11.0	7.0 10.0	4.0 15.0	0.0 21.0	0.0 19.0	0.0 19.0	0.0 19.0	0.0 22.0	0.0 24.6		
	PNB	105.0 91.0	105.0 91.0	105.0 91.0	26.0 91.0	17.0 91.0	0.0 91.0	0.0 91.0	0.0 91.0	0.0 91.0		
$O_{an}=0.3$	max	19.0 19.0	17.0 21.0	16.0 32.0	9.0 38.0	7.0 38.0	3.0 40.0	0.0 38.0	0.0 30.0			
	Q90	17.0 17.0	14.0 18.0	11.0 24.0	6.0 29.4	5.0 29.4	2.0 32.4	0.0 33.0	0.0 29.0			
	mean	13.6 14.2	11.4 16.1	8.4 19.2	3.8 24.2	3.0 24.8	1.0 27.5	0.0 28.1	0.0 25.7			
	Q10	11.0 11.0	10.0 14.0	5.0 15.0	2.0 20.0	2.0 21.0	0.0 23.0	0.0 24.6	0.0 24.0			
	PNB	105.0 91.0	105.0 91.0	105.0 91.0	105.0 91.0	105.0 91.0	77.0 91.0	0.0 91.0	0.0 91.0			
$O_{an}=0.4$	max	22.0 19.0	20.0 22.0	15.0 26.0	11.0 28.0	10.0 28.0	7.0 30.0	2.0 29.0				
	Q90	17.0 15.0	15.0 17.0	11.0 20.0	9.0 23.0	8.0 24.0	5.0 26.0	2.0 27.0				
	mean	13.7 12.5	12.5 14.1	8.7 17.1	6.6 19.9	5.9 20.1	4.1 21.6	0.9 25.5				
	Q10	10.0 10.0	10.0 12.0	7.0 14.0	5.0 18.0	4.0 15.6	3.0 18.0	0.0 24.0				
	PNB	105.0 91.0	105.0 91.0	105.0 91.0	105.0 91.0	105.0 91.0	105.0 91.0	77.0 91.0				
$O_{an}=0.5$	max	16.0 19.0	18.0 21.0	15.0 20.0	14.0 24.0	9.0 21.0	8.0 20.0					
	Q90	14.0 17.0	14.0 17.0	12.0 17.4	12.0 20.0	8.0 19.0	7.0 19.0					
	mean	11.3 13.6	11.4 13.5	10.0 14.5	8.9 15.7	7.2 16.5	6.1 18.5					
	Q10	9.0 11.0	9.0 11.0	8.0 12.0	7.0 13.0	6.0 14.0	5.0 18.0					
	PNB	105.0 91.0	105.0 91.0	105.0 91.0	105.0 91.0	105.0 91.0	105.0 91.0					
$O_{an}=0.6$	max	17.0 18.0	13.0 18.0	14.0 19.0	12.0 17.0	9.0 17.0						
	Q90	14.0 15.4	12.0 16.0	12.0 17.0	11.0 16.0	9.0 16.0						
	mean	11.6 12.7	9.9 14.0	9.9 14.6	9.2 13.7	8.0 15.5						
	Q10	9.0 10.0	8.0 12.0	8.0 13.0	8.0 12.0	7.0 15.0						
	PNB	105.0 91.0	105.0 91.0	105.0 91.0	105.0 91.0	105.0 91.0						
$O_{an}=0.7$	max	15.0 17.0	12.0 15.0	11.0 15.0	10.0 15.0							
	Q90	13.0 15.0	11.0 14.0	11.0 15.0	10.0 15.0							
	mean	11.0 12.6	9.8 12.8	9.6 13.3	9.3 14.5							
	Q10	9.0 11.0	9.0 12.0	9.0 12.0	9.0 14.0							
	PNB	105.0 91.0	105.0 91.0	105.0 91.0	105.0 91.0							
$O_{an}=0.8$	max	13.0 14.0	12.0 15.0	11.0 15.0								
	Q90	12.0 13.4	11.0 14.0	11.0 14.0								
	mean	10.6 12.3	10.2 12.8	10.1 13.4								
	Q10	9.0 11.0	9.0 12.0	10.0 13.0								
	PNB	105.0 91.0	105.0 91.0	105.0 91.0								
$O_{an}=0.9$	max	12.0 14.0	12.0 13.0									
	Q90	12.0 13.0	11.0 13.0									
	mean	10.6 12.4	10.5 12.7									
	Q10	10.0 12.0	10.0 12.0									
	PNB	105.0 91.0	105.0 91.0									
$O_{an}=1$	max	12.0 13.0										
	Q90	11.0 12.0										
	mean	11.0 12.0										
	Q10	10.0 11.6										
	PNB	105.0 91.0										

Fig. 8. Results for experiment 3. The parameter O_{angle} is calculated by $O_{angle} = 1 - O_{FER} - O_{FDI}$.

Since this algorithm setting has up to 5 values that influence the entire monitoring process, we decided to conduct a parametric study for the following range of parameters:

- O_{FER} - pheromone influence in the range of 0 to 1 with a step of 0.05;
- O_{FDI} - influence of the FDI index in the range of 0 to $1 - O_{FER}$ with a step of 0.05;
- o_{angle} - influence of the angle by which it must rotate $o_{angle} = 1 - O_{FER} - O_{FDI}$;
- OV - ratio of pheromone degradation $OV * FDI_i$ in the range 0.01 to 0.34 with a step size of 0.03;
- FR - value of pheromone added to a given point in the range 100 to 500 with a step size of 50.

Each simulation was set for a duration of 20000 seconds, with agents moving at a constant speed of 5 m/s. For each experiment (a given combination of parameters O_{FER} , O_{FDI} , o_{angle}), five repetitions were performed and the arithmetic mean of the individual values was calculated. This experiment was performed in an environment where the space was divided into two contiguous parts in a ratio of 55% $FDI = 1$ and 45% $FDI = 3$. Due to the huge number of experiments, we filtered out solutions where both spaces were completely searched and the ratio of median values was in the range of $2.5x - 3.5x$ (which represented 1482 settings) or $2.8x - 3.2x$ (574 settings), and using a classification method, we divided the solutions into groups, evaluating the vector between Q10 and Q90 of a given space (the steeper the vector, the more evenly the space is searched, see Fig. 9 and more detailed best result classified in class 12, Fig. 10). More detailed best results of the class 12, sorted by O_{FER} value is illustrated on the Fig. 11. It can be seen that the influence of the o_{angle} value has very little effect on the monitoring process. The ratio between the pheromone FR and the evaporation sizes OV varies in the range of 3200 ± 400 . This suggests a possible dependence between these parameters.

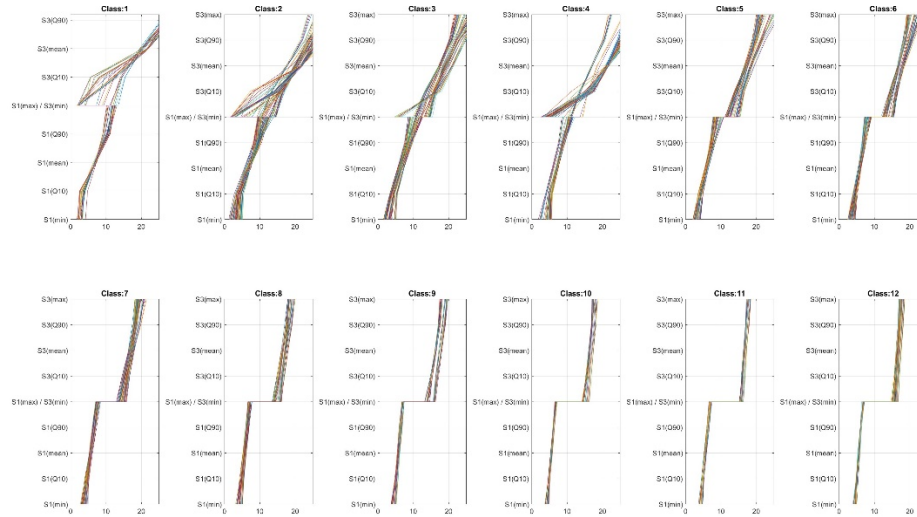


Fig. 9. Classified results of the parametric simulation of the experiment 3 .

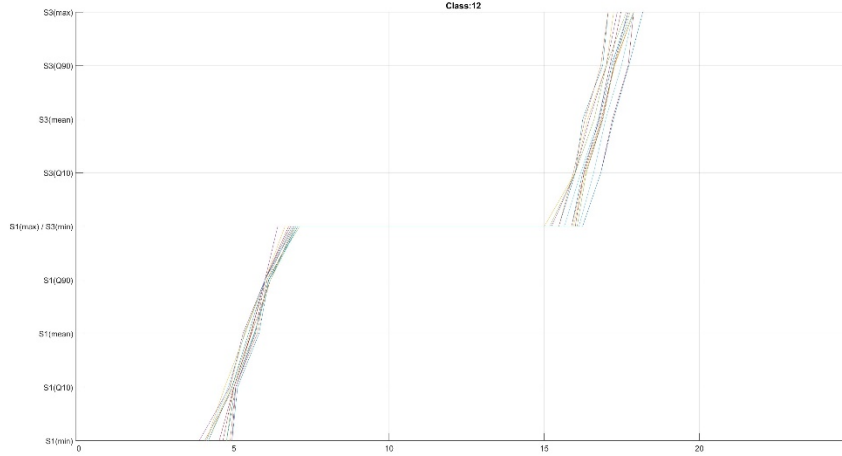


Fig. 10. More detailed best results of the experiment 3.

<i>FER</i>	<i>OV</i>	<i>O_{FER}</i>	<i>O_{FDI}</i>	<i>O_{angle}</i>	ratio	mean FDI=1	mean FDI=3
300	0.1	0.5	0.35	0.15	3.02	5.57	16.84
350	0.07	0.5	0.5	0	3.05	5.73	17.45
450	0.13	0.5	0.45	0.05	3.05	5.64	17.19
350	0.1	0.5	0.45	0.05	3.10	5.56	17.20
400	0.13	0.5	0.4	0.1	3.10	5.57	17.26
300	0.1	0.5	0.4	0.1	3.15	5.47	17.23
450	0.1	0.5	0.5	0	3.16	5.57	17.61
300	0.07	0.5	0.5	0	3.18	5.52	17.58
400	0.1	0.55	0.45	0	2.81	5.95	16.70
450	0.13	0.55	0.4	0.05	2.81	5.95	16.71
500	0.13	0.55	0.45	0	2.86	5.87	16.82
300	0.1	0.55	0.3	0.15	2.88	5.69	16.39
150	0.04	0.55	0.45	0	2.89	5.81	16.78
250	0.07	0.55	0.45	0	2.90	5.83	16.91
400	0.13	0.55	0.35	0.1	2.93	5.70	16.73
350	0.1	0.55	0.45	0	2.96	5.70	16.88
300	0.1	0.55	0.35	0.1	2.96	5.65	16.74
450	0.13	0.55	0.45	0	2.98	5.66	16.89
200	0.07	0.55	0.3	0.15	3.01	5.52	16.61
500	0.16	0.55	0.4	0.05	3.04	5.49	16.73
400	0.13	0.55	0.4	0.05	3.08	5.49	16.88
500	0.16	0.55	0.45	0	3.17	5.35	16.98
500	0.16	0.6	0.35	0.05	2.89	5.69	16.45
400	0.13	0.6	0.35	0.05	2.89	5.66	16.39
500	0.16	0.6	0.4	0	2.97	5.66	16.80
300	0.1	0.6	0.35	0.05	2.99	5.54	16.57
400	0.13	0.6	0.4	0	3.02	5.55	16.76
200	0.07	0.6	0.3	0.1	3.07	5.42	16.62
300	0.1	0.6	0.4	0	3.09	5.41	16.72
500	0.16	0.65	0.35	0	2.84	5.75	16.31
400	0.13	0.65	0.35	0	2.86	5.67	16.24
300	0.1	0.65	0.3	0.05	2.89	5.69	16.46
300	0.1	0.65	0.35	0	3.02	5.46	16.48
300	0.1	0.7	0.3	0	2.90	5.56	16.12
200	0.07	0.7	0.3	0	3.07	5.33	16.40
450	0.16	0.7	0.3	0	3.11	5.29	16.46
300	0.1	0.75	0.25	0	2.82	5.70	16.07
200	0.07	0.75	0.25	0	2.89	5.65	16.36

Fig. 11. More detailed best results of experiment 3, class 12, sorting by *O_{FER}* value and The search ratio between individual areas is colored in a color scale.

3 Conclusion

The results of the third experiment show that the parameters o_{FER} and o_{FDI} have the greatest impact on the overall search of the space (with the provision of a ratio between different FDI areas). The representation of the parameter o_{angle} has only a small to negligible impact on the search process. The coordination process is therefore dependent on the size of the pheromone and the size of the evaporation of this pheromone substance in a given environment. From the results shown in Fig.11, it can be seen that the ratio between the pheromone FR and the evaporation sizes OV varies in the range of 3200 ± 400 . This suggests a possible dependence between these parameters, and they may merge. Presented experiments represent that proposed algorithm achieves a degree of stability and status of covered space (simple or more complex environment). From previous experiments [10] it is clear that pheromone marking supports more efficient and even monitoring of the space, however, with a larger number of robots, conflicts may occur more frequently. Reactions and resolution of conflict situations cause a negative effect, namely slowing down the monitoring process. Therefore, it would be appropriate that some degree of automatic scalability of the group size with respect to the size of the space is also included.

In further research, we will focus on verifying these parameters across different types of environments, not only in terms of size, shape, and distribution, but also with different combinations of FDI values. The experiments will also focus on adjusting the evaporation pattern. Currently the formula (3) is set to linear dependency and works for simple environments, however a combination of different environments can cause local deadlocks if set incorrectly (incorporating the size of the ratio of FDI values into the formula, the size of the area for each FDI, etc., these values can be calculated from the local agent map)

This work was supported by the project SILVANUS-SK (Grant No. 09I01-03-V04-00107), funded through the Recovery and Resilience Plan Mechanism ,VEGA project No. 2/0135/23 and bilateral project Cyber-Physical System for environmental monitoring and data analysis (BAS-SAS-2024-01).

References

1. SILVANUS project homepage, Integrated Technological and Information Platform for Wildfire Management, <https://silvanus-project.eu/> , last accessed 2026/2/11.
2. FCAI web page, <https://fcai.fi/news/2022/8/15/using-drone-swarms-to-monitor-and-combat-future-wildfires?rq=using-drone-swarms-to-monitor>, last accessed 2026/2/11.
3. Zelenka, J, Kasanický, T., Gatila, E., Balogh, Z., Majlingová, A., Brodrechtová, Y., Kalinová, S., Reháč, R., Semen, Y., Boussu, G., Coordination of drones swarm for wildfires monitoring. In Proceedings of the International ISCRAM Conference. - ISCRAM, 2023, vol. 20, pp. 144-151. ISSN 2411-3387. <https://doi.org/10.59297/MUJT3755> (20th Global Information Systems for Crisis Response and Management Conference).

4. Zelenka, J, Kasanický, T., Gatila, E., Balogh, Z., Reháč, R., Koordinácia roju bezpilotných prostriedkov pre monitorovanie lesného požiaru pre podmienky lokality SK a CZ. In Požární ochrana 2023 : Recenzovaný sborník abstraktů XXXII. ročníku mezinárodní konference. - Ostrava : Sdružení požárního a bezpečnostního inženýrství, z.s., 2023, p. 93-96. ISBN 978-80-7385-267-2. (Požární ochrana 2023 : XXXII. ročník mezinárodní konference.)
5. Steffen, A. D. (2020). Drones are delivering medical supplies to the isle of wight. <https://www.intelligentliving.co/drones-medical-supplies-isle-of-wight/>
6. Puente-Castro, A., Rivero, D., Pazos, A. et al. (2022), A review of artificial intelligence applied to path planning in UAV swarms. *Neural Comput & Applic* 34, 153–170 (2022). <https://doi.org/10.1007/s00521-021-06569-4>
7. Tzoumas, G., Pitonakova, L., Salinas, L. et al. (2022) Wildfire detection in large-scale environments using force-based control for swarms of UAVs. *Swarm Intell.*, <https://doi.org/10.1007/s11721-022-00218-9>
8. L. R. Salinas, G. Tzoumas, L. Pitonakova and S. Hauert, "Digital twin technology for wildfire monitoring using UAV swarms," 2023 International Conference on Unmanned Aircraft Systems (ICUAS), Warsaw, Poland, 2023, pp. 586-593, doi: 10.1109/ICUAS57906.2023.10155819.
9. Saffre, F.; Hildmann, H.; Karvonen, H.; Lind, T. Monitoring and Cordoning Wildfires with an Autonomous Swarm of Unmanned Aerial Vehicles. *Drones* 2022, 6, 301. <https://doi.org/10.3390/drones6100301>
10. ZELENKA, Ján** - KASANICKÝ, Tomáš - BUNDZEL, Marek - ANDOGA, Rudolf. Self-adaptation of a heterogeneous swarm of mobile robots to a covered area. In *Applied Sciences-Basel*, 2020, vol. 10, no. 10, art. no. 3562. (2020 - Current Contents). ISSN 2076-3417. Dostupné na: <https://doi.org/10.3390/app10103562>
11. Grunwald D., Wawrzyniak M., Przybyszewski M., Gatil E., Balogh Z., Hassankhani-Dolatabadi S. SILVANUS Dashboard for Wildfire Management, (2024), In *Proceedings of the International ISCRAM Conference*. - ISCRAM, 2023, vol. 20, pp. 152-165. ISSN 2411-3387. available at: <https://seafire.sk/f/3fd9e70183434635a158/?dl=1> (20th Global Information Systems for Crisis Response and Management Conference).